Nuclear and Emerging Technologies for Space
Knoxville, TN, April 6 – April 9, 2020, available online at https://nets2020.ornl.gov

FABRICATION OF UN-MO CERMET NUCLEAR FUEL USING ADVANCED MANUFACTURING TECHNIQUES

Alicia M. Raftery[1], Rachel Seibert[1], Daniel Brown[2], Michael Trammell[1], Andrew Nelson[1], and Kurt Terrani[1]

[1]*Oak Ridge National Laboratory, Oak Ridge, TN, 37831*
[2]*X-Energy, Rockville, MD, 20852, 865-576-7882*

Primary Author Contact Information: 865-241-0130, rafteryam@ornl.gov

This paper demonstrates the use of advanced manufacturing techniques to produce ceramic-metallic nuclear fuel pellets with uranium nitride (UN) microspheres encased in a molybdenum (Mo) matrix. Binder jetting is used to print Mo disks that are filled with UN microspheres and afterwards are sintered using spark plasma sintering. Two fuel pellets were fabricated to demonstrate success of the methodology and to provide a baseline analysis of the effects of temperature processing conditions. Characterization of the resulting fuel pellets includes microstructural analysis and thermal conductivity measurements.

I. INTRODUCTION

Ceramic-metallic (CERMET) nuclear fuel consists of ceramic fuel particles embedded in a metal matrix. Interest in CERMET fuels originated in the search for a fuel suitable for use in very high temperature reactors, such as those used in nuclear thermal propulsion (NTP) systems proposed for deep space exploration.[1] The purpose of the metallic matrix is to increase the thermal conductivity and protect the fuel from detrimental interactions with a high temperature coolant. This is especially true in NTP reactors, where hydrogen gas at temperatures up to 2600ºC (2873K) is the proposed coolant.[2] Various CERMET fuel compositions were investigated with promising results in the 1960's, including UO_2-W, UO_2-Mo, UN-W, and UN-Mo.[3,4] In recent years, the emergence of advanced manufacturing technologies has revitalized research and development into fabrication of CERMET fuels.

Advanced manufacturing techniques, or those that use innovative technology to build parts compared to conventional methods, are aggressively being explored for a wide array of fields that utilize materials processing. Spark Plasma Sintering (SPS) is a sintering technique that uses an electrical current to provide heat while simultaneously applying a uniaxial pressure to sinter materials. SPS has been used successfully to fabricate high-density CERMET fuels with properties including enhanced thermal conductivity and controlled grain size.[5,6] Additive manufacturing refers to a subset of advanced manufacturing techniques that are used to build parts on a layer by layer basis. Binder jetting is one technique that uses alternating deposition of binder and powder to create a three-dimensional part and has been used to print a number of different metallic materials.[7] Some type of post-processing step, such as sintering or infiltration, is typically required since the parts are printed with a green density of approximately 40-60% theoretical density (TD), depending on powder feedstock properties.[8] This study demonstrates a route of fabrication using binder jetting of Mo and subsequent SPS to fabricate UN-Mo fuel pellets. The microstructure and thermal conductivity of the pellets are characterized, and recommendations for improvements of fuel properties are made.

II. EXPERIMENTAL

II.A. UN Feedstock

UN microspheres were fabricated via solution-gelation (sol-gel) and conversion at Oak Ridge National Laboratory (ORNL) using a processing methodology previously described in literature.[9-11] The resulting microspheres had an average diameter of 810 μm and a density of 13.60 g/cm^3 (94.89% TD). The carbon content of the UN microspheres was determined to be 9772 ppm, corresponding to a stoichiometry of $UC_{0.2}N_{0.8}$, which is generally considered high for bulk UN fuel but was acceptable for these preliminary studies. Figure 1 (a-c) shows a series of scanning electron microscope (SEM) images of the UN microspheres; energy dispersive spectroscopy (EDS) was used to analyze the material for impurities. Sulfur impurities were detected (Figure 1(c)), the presence of which is likely due to a dispersing agent that is used in the sol-gel process.

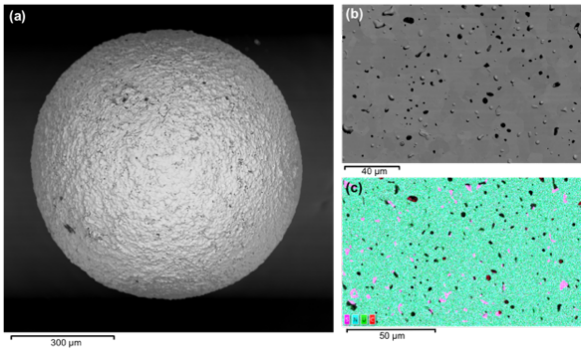

Fig. 1. (a) SEM image of the surface of a UN microsphere, (b) the microstructure showing grains and pores, and (c) the coupled EDS scan showing the presence of sulfur impurities (pink) in the material.

II.B. Binder Jetting Mo

Mo disks were printed using an ExOne Innovent binder jet printer. The Mo feedstock was TEKMAT Mo-45 spherical powder with an average size of 45 µm ± 15µm, an oxygen content < 250 ppm, and a tap density of 5 g/cm^3, according to the manufacturer's specifications.

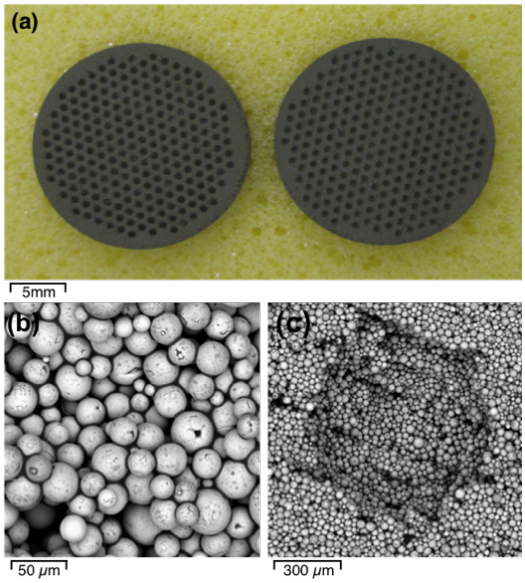

Fig. 2. (a) Photograph of binder jet printed Mo disks, SEM images showing (b) the binder providing particle to particle bonding, and (c) a printed hole for placement of a UN microsphere.

The Mo disks were printed to approximately 20mm in diameter and 2mm in height, with a pattern containing 225 holes located on both sides of the disk for placement of UN microspheres. The disks were printed using an aqueous binder, and immediately after printing were placed in a furnace at 190ºC for 6 hours to cure the binder. After curing, the disks were excavated from the powder bed by removing excess powder; the resulting parts are shown in Figure 2(a). SEM images of the disks indicate good wetting of the binder between Mo particles (Figure 2(b)). In addition, the printed holes for the UN microspheres are not entirely spherical and have rough edges, as seen in Figure 2(c).

II.C. UN-Mo Pellet Fabrication

The SPS system used for sintering was a Thermal Technology SPS 25-10. All materials were loaded into a graphite die, between two graphite punches, with graphite foil surrounding the material both axially, with 0.5mm on top and bottom, and radially, with 0.127mm around the sample. The purpose of the graphite foil is to prevent interaction of the material being sintered with the graphite die and punches at high temperatures. The bottom Mo disk was loaded in the graphite die and one layer of 225 UN microspheres were placed in the disk, with one microsphere per hole. The loaded disk is shown in Figure 3(a). The second Mo disk with the matching pattern was fit on top to hold the microspheres in place. Figure 3(b) shows the graphite die prepared with material and punches. The die was loaded into the chamber between graphite blocks, which aid in centering and provide a pathway of conduction for the current to pass through the die (Figure 3(c)). In addition, graphite felt surrounded the die axially and radially to insulate during sintering.

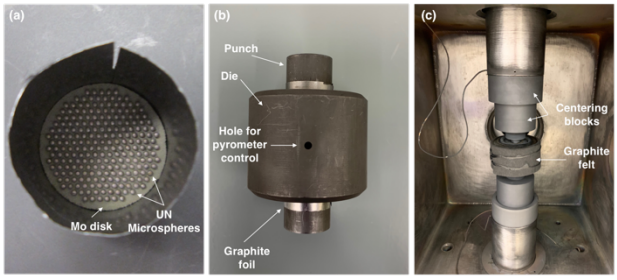

Fig. 3. (a) Photograph of Mo disk placed inside of graphite die and loaded with UN microspheres before sintering, (b) graphite die with punches inserted, and (c) graphite die positioned in SPS stack for sintering.

To ensure consistency between samples, many of the processing parameters were held constant. The vacuum was brought to and held at 2.0 x 10^{-3} Torr and the direct current (DC) pulse was set to 12ms on/2ms off. The temperature ramp rate for heating and cooling was 150ºC/min, and the hold time at maximum temperature was 10 minutes. The pre- and post-pressure was 15 MPa, which ensures good electrical contact between the punches and graphite centering blocks. The sample temperature was measured during the experiments with an optical pyrometer; therefore, the recorded temperatures are representative of the surface temperature of the material being sintered. Two UN-Mo pellets were fabricated at two different temperatures and pressures, as a proof-of-concept and to obtain a baseline analysis of temperature effects.

III. RESULTS

The processing parameters and resulting densities are shown for each pellet in Table I. After sintering, silicon carbide grit paper was used to remove the graphite foil from the fueled pellets. Some residual graphite foil remained, which can be seen on pellet UNMo-1, pictured in Figure 4(a). The pellets were mounted in conductive epoxy and cut aggressively to remove the Mo and reach mid-plane of the microspheres for imaging and analysis. Figure 4(b) shows a photograph of pellet UNMo-1 during metallographic preparation; the UN microspheres are mostly intact, but a small number have cracked, which is either a result of pressure during sintering or material pullout during sample preparation. Figure 4(c) is an x-ray radiograph of pellet UNMo-2, showing the UN microspheres distributed evenly throughout the Mo matrix.

TABLE I. Results for two UN-Mo pellets made, showing the SPS processing conditions and resulting densities.

Pellet ID	Temperature [ºC]	Pressure [MPa]	%TD
UNMo-1	1600–1650	25–35	71.97
UNMo-2	1650–1700	55–65	92.31

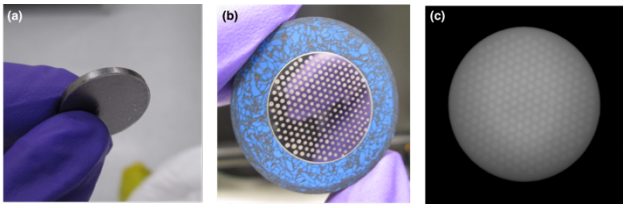

Fig. 4. (a) Photograph of pellet UNMo-1 after sintering, (b) during metallographic preparation, and (c) an x-ray radiograph of pellet UNMo-2, showing UN microspheres distributed throughout the Mo matrix.

III.A. Microstructural Characterization

The pellets were polished to a finish suitable for electron backscatter diffraction (EBSD) and imaged using a TESCAN MIRA3 GHM SEM. The primary features of interest were the grain size, the thickness and composition of interaction layers, and the presence of any secondary phases or impurities. Figures 5(a,b,d,e) show optical and SEM overviews of UN microspheres located within the Mo matrix of each pellet, highlighting the varying level of densification between the two pellets. Figures 5(c,f) show a similarity in grain structure and grain size in the UN regions between the two pellets. The grain structure in the Mo regions differs between the pellets due to the different levels of densification, but on the whole the matrix Mo grains are larger than those observed in the UN.

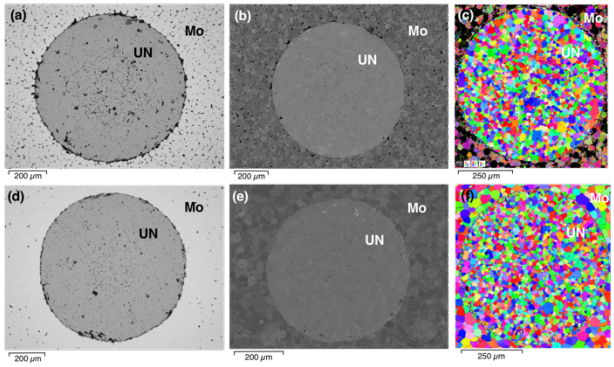

Fig. 5. (a) Optical image, (b) SEM image, and (c) EBSD band contrast map of the cross section of selected UN microspheres from pellet UNMo-1 and (d) optical image, (e) SEM image and (f) EBSD band contrast map of selected UN microspheres from pellet UNMo-2.

Figures 6(a-d) show the UN-Mo interface for each pellet. There is a continuous crack along the perimeter of the UN microsphere between the UN and the Mo regions in both pellets. The crack width ranges from 1–30µm in UNMo-1, with the large range due to the Mo particles only necking around the microsphere, leaving gaps between particles. The crack size around the UN microspheres in UNMo-2 is consistently < 2µm. The cracks in both pellets are most likely explained by the higher coefficient of thermal expansion in UN compared to Mo, resulting in its shrinkage during cooldown. There was no interaction phase observed at the boundary between the UN and Mo in either pellet.

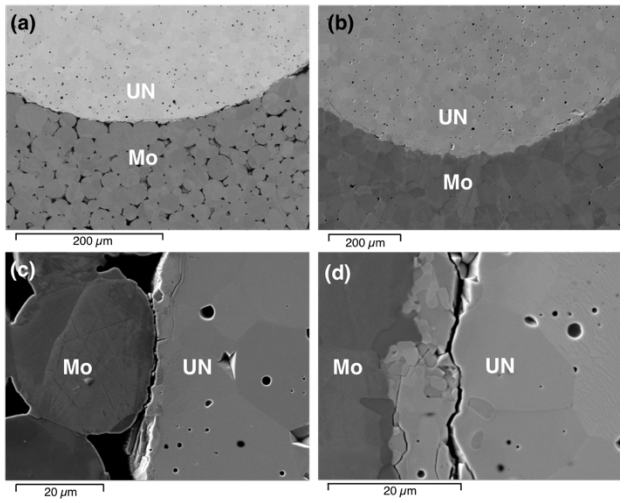

Fig. 6. Overview of UN-Mo interface for (a) pellet UNMo-1 and (b) pellet UNMo-2, and close-up of the interface for (c) UNMo-1 and (d) UNMo-2.

It was expected that carbon diffusion from the graphite foil surrounding the pellet during sintering would form an interaction layer along the perimeter of the pellet, since this is observed in many materials that are processed using SPS. The presence of a carbide layer was confirmed in each pellet and was characterized using EBSD to be Mo_2C. Figures 7(a,b) show a comparison of the interaction layer between the two pellets; the thickness was measured to be approximately 80–100µm in UNMo-1 and 100–140µm in UNMo-2. The difference in thickness is likely due to the higher temperature used during fabrication of UNMo-2.

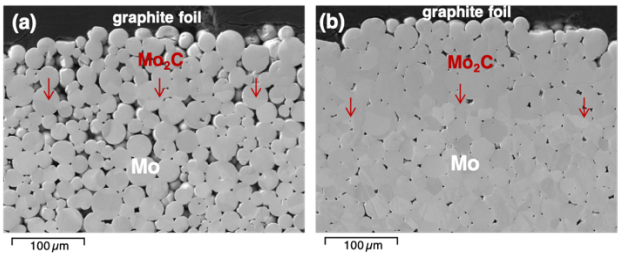

Fig. 7. Interface between graphite foil and Mo regions in (a) UNMo-1 and (b) UNMo-2, showing the carbide layer resulting from interaction with the graphite foil.

An EDS map scan of the UN microspheres revealed an oxide layer surrounding each sphere, which is shown for a microsphere in UNMo-1 in Figure 8. The oxide was present at the same thickness (~8µm) on the perimeter of

each microsphere in both pellets. The oxide formation is likely a result of the feedstock being stored in air for an extended period of time before being used in this study. No other significant impurities or secondary phases were found in the pellets.

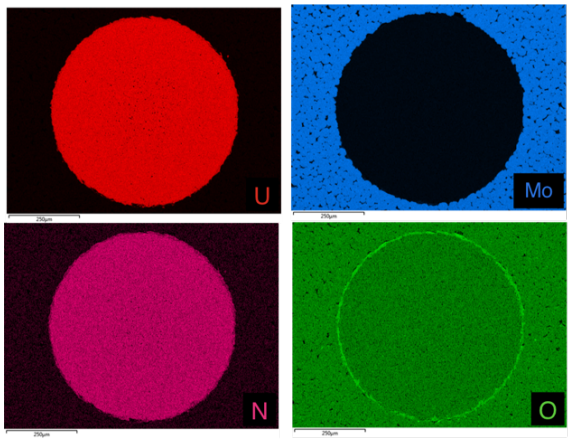

Fig. 8. EDS map results for UN microsphere located in UNMo-1, showing an oxide layer on the perimeter of the microsphere.

III.B. Thermal Conductivity

Thermal diffusivity measurements were made using a Netzsch LFA 475 MicroFlash instrument. The thermal diffusivities of UNMo-1 and UNMo-2 were measured as a function of increasing temperature. Measurements were recorded every 50ºC from room temperature (25ºC) to 900ºC. Figure 9 shows the results converted to thermal conductivity, along with reference values for Mo and UN fabricated via conventional routes.[12,13]

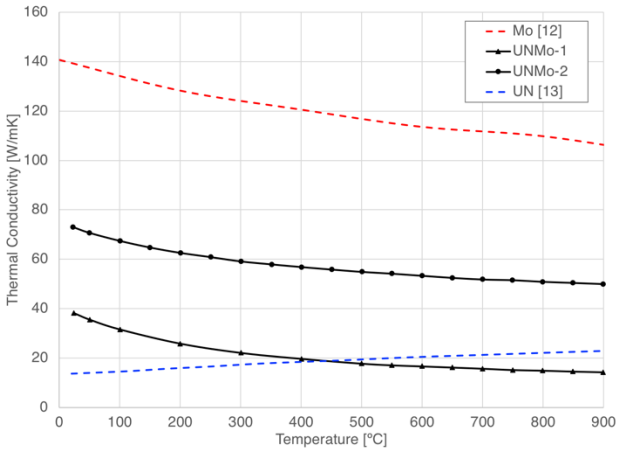

Fig. 9. Thermal conductivity results for UNMo-1 and UNMo-2, as well as reference values for Mo and UN fabricated via conventional routes.[12,13]

UMo-2 has higher values for thermal conductivity across all temperatures when compared to UNMo-1, which is due to the higher density in the Mo region. There is an increase in the thermal conductivity of both pellets with respect to reference values for UN, but a significant decrease compared to the reference values of Mo. The reduction is likely due to the trapped porosity within the disks, as well as the lower thermal conductivity contribution from the UN.

IV. CONCLUSIONS

This paper describes the fabrication of UN-Mo CERMET nuclear fuel using a route that utilizes advanced manufacturing techniques. Characterization of the two pellets showed results that are consistent with those expected from the two temperature processing conditions and resulting densities. Notably, the high-density pellet showed an enhanced thermal conductivity compared to monolithic UN fuel while featuring a full encapsulation of the UN fuel microspheres within a densified Mo matrix. Both properties are advantageous when considering this fuel for use in high temperature systems.

Adverse pellet properties include cracking of some microspheres and the formation of a carbide interaction layer at the perimeter of the pellet, both of which have the potential to be mitigated by altering the processing parameters. Modifications that would improve the fuel properties of the UN-Mo fuel design specific to this work include increasing the fuel volume fraction with slight changes to the Mo disk design. For instance, the disks could be made thinner with holes printed only on one side to minimize porosity and maximize the fuel volume fraction. The ease with which these changes could be implemented using the binder jetting technique is a testament to the versatility of this processing methodology.

Perhaps most significant in this work is the demonstration of a novel fabrication methodology, which proves the ability to spatially place fuel inside of a matrix using a combination of advanced manufacturing techniques. This innovation has far-reaching implications in terms of expanding the nuclear fuel design space. It is reasonable to conclude that these techniques will provide the ability to achieve fuel geometries, compositions, and properties outside of the realm of current traditional manufacturing techniques.

ACKNOWLEDGMENTS

The authors would like to acknowledge Rodney Hunt and Jake McMurray for their contributions in producing the UN feedstock materials and Austin Schumacher for his initial efforts in design. Desarae Godsby and Derek Siddel are recognized for producing the binder jetted Mo parts at the Manufacturing Demonstration Facility (MDF). Lastly, Jeff Pryor, Stephanie Curlin, and Hsin Wang are acknowledged for their efforts in characterization. This work was supported by the Transformational Challenge Reactor (TCR) under the auspices of the U.S. Department of Energy, Office of Nuclear Energy.

REFERENCES

1. S.K. BOROWSKI, D.R. MCCURDY, and T.W. PACKARD, "Nuclear Thermal Propulsion (NTP): A proven growth technology for human NEO/Mars exploration missions," *IEEE Aerospace Conference Proceedings*, 1-20 (2012).
2. WALLACE, T.C. "Review of Rover element protective coating development at Los Alamos," *AIP Conference Proceedings*, 217, 1024-1036 (2008).
3. PAPROCKI, S.J., KELLER, D.L., CUNNINGHAM, G.W., KIZER, D.E., *Preparation and properties of UO2 CERMET fuels*, BMI-1487, Battelle Memorial Institute: Columbus, OH (1960).
4. TAKKUNEN, P.D., *Fabrication of CERMETS of uranium nitride and tungsten or molybdenum from mixed powders and from coated particles*, NASA TN D-5136, Lewis Research Center: Cleveland, OH (1969).
5. BUCKLEY, J., TURNER, J.D, and ABRAM, T.J., "Uranium dioxide – molybdenum composite fuel pellets with enhanced thermal conductivity manufactured via spark plasma sintering," *J. Nucl. Mater.*, 433, 50-54 (2013).
6. O'BRIEN, R., and JERRED, N.D., "Spark plasma sintering of W-UO2 cermets," *J. Nucl. Mater.*, 433, 50-54 (2013).
7. SACHS, E., CIMA, M. and CORNIE, J., "Three-dimensional printing: rapid tooling and prototypes directly from a CAD model." *CIRP Annals*, 39, 201-204 (1990).
8. BAI, Y., WAGNER, G., and WILLIAMS, C.B., "Effect of particle size distribution on powder packing and sintering in binder jetting additive manufacturing of metals," *J. Manuf. Sci. Eng. Trans. ASME*, 139, 1-6 (2017).
9. HUNT, R.D., and COLLINS, J.L., "Uranium kernel formation via internal gelation," *Radiochim. Acta*, 92, 909-915 (2004).
10. LINDEMER, T.B., et al., "Quantification of process variables for carbothermic synthesis of $UC_{1-x}N_x$ fuel microspheres," *J. Nucl. Mater.*, 483, 176-191 (2017).
11. MCMURRAY, J.W., KIGGANS, J.O., HELMREICH, G.W., and TERRANI, K.A., "Production of near-full density uranium nitride microspheres with a hot isostatic press," *J. Am. Ceram. Soc.*, 101, 4492-4497 (2018).
12. ZINOV'EV, V.E., "Thermal properties of metals at high temperatures," *Metallurgiya* (1989).
13. HAYES, S.L, THOMAS, J.K., and PEDDICORD, K.L., "Material property correlations for uranium mononitride," *J. Nucl. Mater.*, 171, 289-299 (1990).